The Implications of Atmospheric 3D Thermal Structure and Clouds on 1D Retrieval

NEW YORK UNIVERSITY ABU DHABI

3D Thermal Structure

Jasmina Blecic, Ian Dobbs-Dixon, Thomas Greene

METHODOLOGY

Using the atmospheric structure from a 3D global radiation-hydrodanamic simulation of HD189733b [1], Figure 1, and the open-source Bayesian Atmospheric Radiative Transfer (BART) code [2][3], Figure 3, we investigate the difference between the temperature structure produced with a 3D simulation and the best-fit 1D retrieved model. We explore how well the retrieved planet-averaged model matches realistically complex atmospheric structure and what temperature-pressure profile is actually revealed by the retrieval.

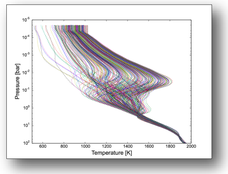

Figure 1: T-P profiles of the HD 189733b dayside produced using [1], sampled on every 10 degrees latitude and longitude

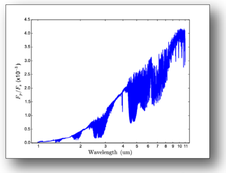

Figure 2: Dayside-integrated emission spectra of HD189733b

Figure 2 shows the high-resolution dayside-integrated emergent model spectra generated using the T-P profiles from Figure 1 in radiative transfer, and the stellar grid model from [4]. To generate synthetic observations and uncertainties of JWST (NIRISS, NIRCam, NIRSpec, and MIRI LRS), HST (WFC3 G141), and Spitzer (IRAC), we use a suit of observational tools by [5], Table 1. The software accounts for the expected exposure, the realistic noise (photon, detector, read noise and dark current, observatory background, and residual systematic noise components), and instrumental throughputs.

Instrument	Mode	Optics	λ (μm)	Native resolution	Sampling (pixels)
NIRISS	Bright SOSS	GR700XD	1.0 – 2.5	700	25
NIRCam	LW grism	F322W2	2.5 – 3.9	1700	2
NIRCam	LW grism	F444W	3.9 – 5.0	1700	2
MIRI	SLITLESS	LRS prism	5.0 – 11.0	100	2

RESULTS

The synthetic data are generated by binning the 3D models over the wavelength range between 1 - 11 μm, where most spectroscopically active species have pronounced features. The data with uncertainties are then used as inputs for retrieval. In Figure 4, we show data points and uncertainties for all instruments together.

To compare the 3D T-P structure with the results from retrieval, we first included all synthetic data points and uncertainties for JWST, HST and Spitzer together and then we address each of them separately, Figure 5 and 6.

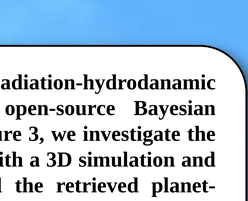

Figure 4: Simulated data for JWST, HST, and Spitzer

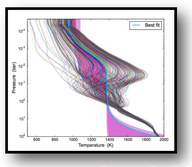

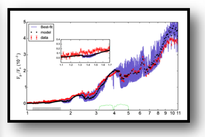

Figure 5: JWST, HST, and Spitzer

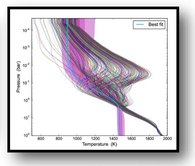

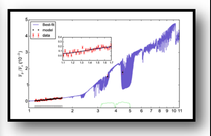

Figure 6 : HST and Spitzer

Retrieval

See poster by Patricio Cubillos

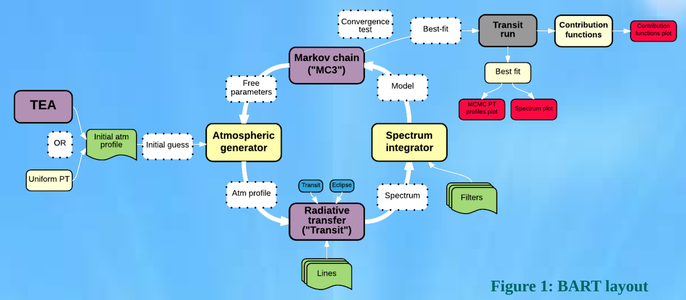

Figure 1: BART layout

PYRAT BAY

Pyrat Bay [6] is an open-source retrieval framework based on the BART code [2][3], Figure 1. We rewrote the complex object-oriented core of the BART code from C to Python, making the new framework simpler to debug, edit, and built upon. The code is user and developer friendly, accompanied with detail documentation https://pcubillos.github.io/pyratbay/. As BART, Pyrat Bay consists of three self-consistent modules: Thermochemical Equilibrium Abundances (TEA) module https://www.github.com/dzesmin/TEA [7], radiative-transfer module, and Multi-core Markov-chain Monte Carlo module (MC3) https://www.github.com/pcubillos/MCcubed [8]. The object-oriented structure and the driver routine based on a set of configuration files allow user to run the code in stages and call back variables with no additional editing.

REFERENCES

[1] Dobbs-Dixon et al., 2013, MNRAS, 435, 3159
[2] Blecic 2016, arXiv:1604.02692
[3] Cubillos 2016, arXiv:1604.02692
[4] Castelli et al., arXiv:astro-ph/0405087
[5] Greene et al., 2016, ApJ, 817, 17
[6] Cubillos et al., in prep
[7] Blecic et al., 2016, ApJS, 225, 4
[8] Cubillos et al., submitted
[9] Ackerman and Marley 2001, ApJ, 556, 872
[10] Benneke 2015, arXiv:1504.07655B
[11] Dave, 1968, IBM SC, Rp # 320-3236
[12] Toon and Ackerman, 1981, App. Op., 20, 3657

CONTACT

New York University
Abu Dhabi
Post-Doctoral Associate

JASMINA BLECIC
jasmina@nyu.edu
https://github.com/dzesmin/

Cloud Models

Jasmina Blecic, Ashley Baker, Mark Marley, Patricio Cubillos, Ian Dobbs-Dixon

METHODOLOGY

To address clouds in our models, we implement a cloud parameterization inspired by the 1D cloud model of [9] and the analytical cloud profile shape by [10], Figure 7. Our cloud profile has three free parameters (q_*, p_{top}, H_c) that covers a variety of profile shapes observed and modeled for Solar System planets, brown dwarfs and exoplanets, in addition to a gray cloud model, Figure 8:

$$q_c(p) = q_* \left(\log p - \log p_{top}\right)^{H_c} \qquad p_{top} \le p < p_{base}$$

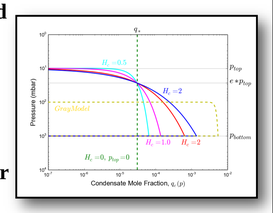

Figure 8: Cloud profile

where q_c is the condensate number fraction, q_* is the condensate number fraction one scale height below the cloud top and H_c is the cloud profile shape factor.

We calculate the cloud base as an intersection between our T-P profile and the species vapor pressure curve, Figure 9.

The particle size distribution is described by a log-normal distribution [9], adding an additional free parameter r_g to our model, Figure 10:

$$\frac{dn}{dr} = \frac{N}{r\sqrt{2\pi}\,log\sigma_g}\,exp\left[-\frac{log^2\left(r/r_g\right)}{2log^2\sigma_g}\right] \qquad N = \frac{q_c\,\varrho_{H_2}}{norm}$$

where r_g, the geometric mean radius of the particles, σ_g geometric mean radius set to 2.

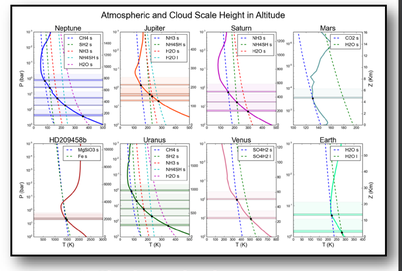

Figure 9: Cloud extend and vapor pressure curves

To calculate extinction due to the cloud particles, we use Mie scattering theory [9] [11] [12], which outputs scattering and absorption efficiencies Q_{scat} and Q_{abs} of each condensate for the range of particle sizes and wavelengths. The cloud cross sections and extinction are calculated as:

$$C_{ext}(\lambda, r) = Q_{scat}(\lambda, r)\pi r^2 + Q_{abs}(\lambda, r)\pi r^2$$

$$ec(\lambda) = \sum_r n(r) C_{ext}(\lambda, r)$$

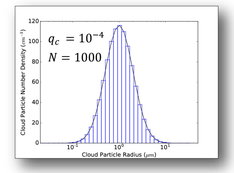

Figure 10: Log-normal distribution

where $n(r)$ is the log-normal distribution weighting function. Figures 11, 12, and 13 show the water absorption, and the extinction efficiencies, and cross sections of water and iron condensates respectively. Figures 15 and 16 show comparison models with and without clouds for Earth and HD209458b.

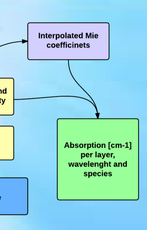

Figure 7: Layout of the cloud code

RESULTS

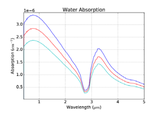

Figure 12: H2O absorption

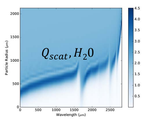

Figure 13: H2O condensates extinction efficiency

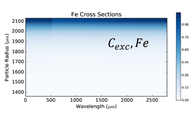

Figure 14: Fe condensates cross sections

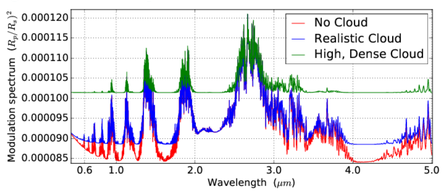

Figure 15: Earth in transmission spectra with and without H_2O clouds

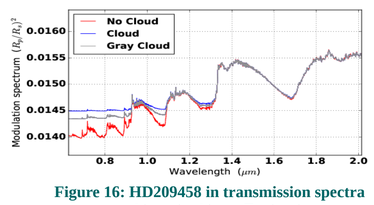

Figure 16: HD209458 in transmission spectra with and without Fe clouds